

PAPER • OPEN ACCESS

Heavy ion irradiation induced failure of gallium nitride high electron mobility transistors: effects of *in-situ* biasing




To cite this article: Md Abu Jafar Rasel *et al* 2023 *J. Phys. D: Appl. Phys.* **56** 305104

View the [article online](#) for updates and enhancements.

You may also like

- [Effect of Heat Treatment on Carbon Supported PtAu Based Bimetallic Nanomaterials for Improved Glucose Sensitivity and Electrocatalytic Performance](#)
Baljit Singh and Eithne Dempsey
- [Not so loosely bound rare gas atoms: finite-temperature vibrational fingerprints of neutral gold-cluster complexes](#)
Luca M Ghiringhelli, Philipp Gruene, Jonathan T Lyon *et al.*
- [Isomerism effects in relaxation dynamics of Au₂₄\(SR\)₄₆ thiolate-protected gold nanoclusters](#)
Yuanze Sun, Xueke Yu, Pengye Liu *et al.*

Heavy ion irradiation induced failure of gallium nitride high electron mobility transistors: effects of *in-situ* biasing

Md Abu Jafar Rasel¹, Ryan Schoell², Nahid Sultan Al-Mamun¹, Khalid Hattar^{2,3}, C Thomas Harris² , Aman Haque^{1,*} , Douglas E Wolfe⁴, Fan Ren⁵ and Stephen J Pearton⁶ 

¹ Department of Mechanical Engineering, Penn State University, University Park, PA 16802, United States of America

² Sandia National Laboratories, Albuquerque, NM 87185, United States of America

³ Department of Nuclear Engineering, University of Tennessee, Knoxville, TN 37998, United States of America

⁴ Department of Materials Science & Engineering, Penn State University, University Park, PA 16802, United States of America

⁵ Department of Chemical Engineering, University of Florida, Gainesville, FL 32611, United States of America

⁶ Department of Material Science and Engineering, University of Florida, Gainesville, FL 32611, United States of America

E-mail: mah37@psu.edu

Received 7 March 2023, revised 8 April 2023

Accepted for publication 24 April 2023

Published 9 May 2023



CrossMark

Abstract

While radiation is known to degrade AlGaIn/GaN high-electron-mobility transistors (HEMTs), the question remains on the extent of damage governed by the presence of an electrical field in the device. In this study, we induced displacement damage in HEMTs in both ON and OFF states by irradiating with 2.8 MeV Au⁴⁺ ion to fluence levels ranging from 1.72×10^{10} to 3.745×10^{13} ions cm⁻², or 0.001–2 displacement per atom (dpa). Electrical measurement is done *in situ*, and high-resolution transmission electron microscopy (HRTEM), energy dispersive x-ray (EDX), geometrical phase analysis (GPA), and micro-Raman are performed on the highest fluence of Au⁴⁺ irradiated devices. The selected heavy ion irradiation causes cascade damage in the passivation, AlGaIn, and GaN layers and at all associated interfaces. After just 0.1 dpa, the current density in the ON-mode device deteriorates by two orders of magnitude, whereas the OFF-mode device totally ceases to operate. Moreover, six orders of magnitude increase in leakage current and loss of gate control over the 2-dimensional electron gas channel are observed. GPA and Raman analysis reveal strain relaxation after a 2 dpa damage level in devices. Significant defects and intermixing of atoms near AlGaIn/GaN interfaces and GaN layer are found from HRTEM and EDX analyses, which can substantially alter device characteristics and result in complete failure.

* Author to whom any correspondence should be addressed.



Original content from this work may be used under the terms of the [Creative Commons Attribution 4.0 licence](https://creativecommons.org/licenses/by/4.0/). Any further distribution of this work must maintain attribution to the author(s) and the title of the work, journal citation and DOI.

Keywords: gallium nitride, high electron mobility transistors, heavy ion irradiation, transmission electron microscopy

(Some figures may appear in colour only in the online journal)

1. Introduction

From sea level to outer space, atmospheric neutrons to highly energetic particles such as protons, electrons, and heavier particles, constantly bombard electronic devices. They generate different effects ranging from both soft effects, such as corruption of the information stored or memory bit flips to irreversible catastrophic burnout of power transistors [1]. The radiation-harsh environment is not limited to only space missions and military applications; in facilities such as nuclear power plants or particle accelerators, even for standard terrestrial operation, radiation can threaten day-to-day operation.

There is a growing tendency to use AlGaIn/GaN high electron mobility transistors (HEMTs) due to the associated potential in high-power, high-temperature, and high-frequency applications. HEMTs are also attractive for high-altitude or space related applications [2], higher threshold energy for atomic displacement [3], and higher dynamic annealing rate enhance radiation tolerance [4]. Due to its high-power density, the presence of thermomechanical stress and high channel temperature are already recognized performance bottlenecks for GaN HEMTs. A large electric field appears under the gate edge across the barrier in the AlGaIn/GaN HEMTs, adding to the existing substantial intrinsic tensile strain at the interface due to lattice mismatch [5]. To make matters worse, ionizing and non-ionizing radiation may significantly impact the device's performance as well [2, 6]. The most common trend is to study radiation effects on devices at the OFF state, ignoring the stressors originating from the operational conditions and the combined effect of irradiation. Therefore, a thorough examination of the combinatorial impact of superimposed radiation environmental stressors and operating stressors on devices is required.

GaN is very radiation tolerant and requires high amounts of exposure to cause alterations, according to preliminary studies on the impacts of radiation on GaN technology [7]. The literature contains studies of heavy ion ((starting with Si)) testing using Iron (Fe), Bromine (Br), Neon (Ne), Argon (Ar), Krypton (Kr), Xenon (Xe), Gold (Au), and Bismuth (Bi) at energy levels ranging from 1.5 MeV to 1.217 GeV [8–12]. Cosmic rays and solar flares are examples of high-energy particles, with heavier ions having energies up to 10 GeV [11]. Damage mechanism by these heavy ions is a function of radiation type, flux, fluence, energy, and temperature, as well as the device specifics such as carrier density, bond energy, material specific heterostructures (AlGaIn/GaN, AlN/GaN or InAlN/GaN), device structure, impurity content, and dislocation density in the GaN-based structure [7, 13, 14]. Due to the increased surface state density of GaN and the lack of a gate dielectric in the HEMT structure, ionization effects in GaN are not as severe as they are in CMOS devices [15]. The degradation of AlGaIn/GaN HEMT devices under ion radiation was attributed to displacement damage caused by the nonionizing

energy-loss of nuclear collisions, while electronic energy-loss processes play a negligible role in defect formation [16]. However, swift, heavy ion radiation with energy in the high MeV and GeV range typically loses energy through electronic interactions in the target. This significant ionization spike acts as a hot electron gas that dumps its energy into lattice by electron-phonon interaction. Sequeira *et al* have demonstrated with 185 MeV gold irradiation that this sudden considerable energy from ionization can induce high temperatures and create a molten tract in the path [16]. Most previous publications focused on the effects of protons, neutrons, and low-to-medium energy ions [14]. It is known that 1.8 MeV light ion (proton) irradiation at $\sim 10^{14}$ protons cm^{-2} fluence decreases in 2-dimensional electron gas (2DEG) mobility by >30%, 2DEG sheet carrier density by 10%, transconductance and saturation current by 68% and 62%, respectively [17, 18]. Gold heavy ions with mid-level energy (1.5 MeV) and 6.5×10^{15} gold cm^{-2} fluence are shown to generate defect clusters that decrease saturation current by four orders of magnitude and cause loss of gate control [12]. Some studies claimed that the presence of an electric field has no impact on incoming ion radiation [19], whereas others show dissimilar behavior in transport properties between ON and OFF conditions [20–24]. Ionizing sources, such as X-ray and ^{60}Co , have been employed to evaluate the influence of irradiation at various bias conditions in HEMTs. Variations of electrical characteristics during gamma irradiation as a function of device structure and bias settings (high gate and drain voltage) have been reported [23]. Another study demonstrated that GaN HEMTs have less susceptibility to 10 KeV x-ray irradiation when in the ON-state and exhibited excellent recovery of functionality after 350 Krad total ionizing dose (TID) [22]. These findings indicate better performance of the HEMTs in the ON-state compared to the OFF-state. This is due to the influence of both vertical and horizontal electric field components, which minimizes the effects of radiation on the dynamics of trapped charges. The effects of proton and x-ray irradiation, as well as hot carrier stress, were also studied for TID and displacement damage effects [24]. The study found that the magnitude of the effects varied significantly with applied bias during exposure and that a single worst-case bias condition cannot be defined for all varieties of AlGaIn/GaN HEMTs. The lack of systematic research on heavy ion irradiation that takes into account the operating state of devices (ON or OFF state) during irradiation, which can substantially influence reliability and tolerance to incoming irradiation [20], is the primary motivation for this study.

2. Materials and methods

Commercially available Cree multi-finger HEMTs (CGH60008D, Wolfspeed, rated at 6 W, 18 GHz, and 40 V)

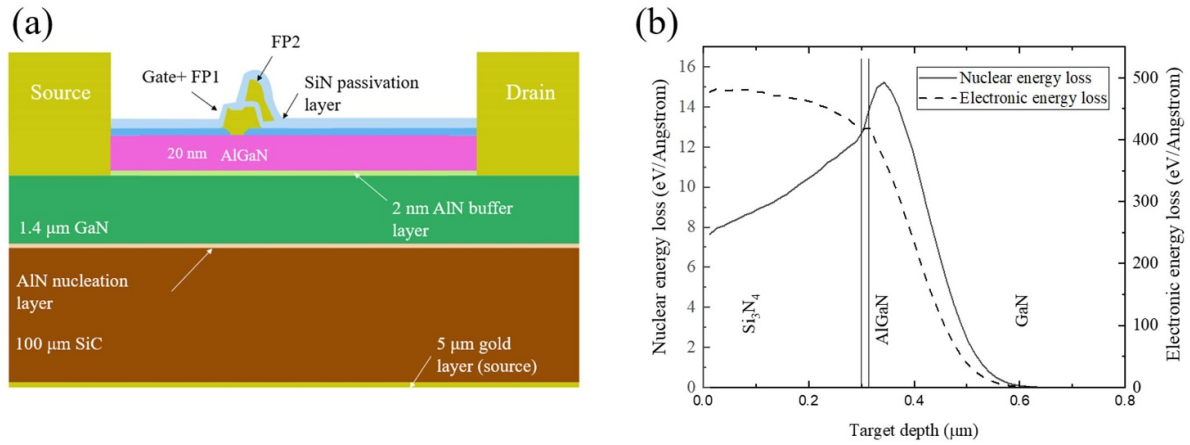


Figure 1. (a) Schematic (not to scale) of the cross-section of GaN HEMT (b) Range of 2.8 MeV gold ion and stopping power of electronic and nuclear interactions.

dies are fabricated with metal–org chemical vapor deposition growth in a high-volume reactor on 100 mm semi-insulating 4 H silicon carbide substrates. Ohmic contacts (Ti/Al/Ni/Au) are formed directly on the top AlGaIn layer, and Schottky metal gate electrodes are formed by recessing through the first SiN dielectric to the AlGaIn and then depositing Ni/Pt/Au metallization. The gate electrode is laterally extended with gate metallization to reshape and redistribute the strong peak electric fields at the drain-side edge. Further electric field shaping is achieved by fabricating a source-connected second field plate (FP2) after the second passivation layer [25]. The layer structure reported by the manufacturer is depicted in figure 1(a), which shows a ≈ 20 nm $\text{Al}_{0.22}\text{Ga}_{0.78}\text{N}$ barrier, ≈ 1 nm thick AlN interlayer, $1.4 \mu\text{m}$ GaN buffer, and $100 \mu\text{m}$ 4H–SiC substrate with a gate length of $L_g = 0.25 \mu\text{m}$.

The Ion Beam Laboratory at Sandia National Laboratories has developed an I³TEM (*In situ* Ion Irradiation TEM) system connected to a 6 MV tandem accelerator [26]. In the beamline, before connecting to the TEM chamber, there is a small chamber suited for irradiating bulk samples and heating, biasing for exploring coupled extreme environments. The devices are irradiated with 2.8 MeV gold ion (Au^{4+}) at the flux of 1.8×10^{10} ions $\text{cm}^{-2} \text{s}^{-1}$ with or without an internal electrical field (ON and OFF mode). Two GaN devices, for ON and OFF states, are wire bonded to a ceramic chip connecting to external Keithley 2400 SMUs to supply voltage during ON mode and *in situ* measurement after specific 2.8 MeV Au^{4+} fluence at both ON and OFF mode operation. During ON mode, devices are operated at $V_{ds} = 2$ V and $V_g = -2$ V with a drain current density of 167 mA mm^{-1} inside the radiation chamber to get both vertical and horizontal electric fields in the devices. The absence of supplementary thermal packaging for this device necessitates the selection of this biasing condition to ensure safe operation within a vacuum chamber without any damage to wire bond connections. The ex-situ ion irradiation was performed on both ON and OFF mode devices at seven different fluence levels: 1.72×10^{10} , 1.72×10^{11} , 1.72×10^{12} , 5.18×10^{12} , 1.21×10^{13} , 1.72×10^{13} , and 3.7×10^{13} ions cm^{-2} . All the ions were at a nominally normal incidence, and all the tests

were performed at room temperature. The stopping and range of ions in matter (SRIM) simulation with the Kinchin–Pease model [27] has been used to calculate the device’s damage level. Irradiation damage levels for each fluence level were 0.001, 0.01, 0.1, 0.3, 0.5, 0.7, 1, and 2 displacement per atom (dpa). We used dpa per volumetric slices as a metric for vacancy production as a function of depth. However, it does not take into consideration factors such as time dependence of defect production, point defect spatial distribution, defect migration & reaction, and defect clustering. From SRIM, we see that the ion range is $0.62 \mu\text{m}$ (figure 1(b)), and the vacancy/damage peak occurs near the 2DEG layer, the conducting channel of the GaN HEMTs, which is why 2.8 MeV energy was chosen for the heavy ion irradiation. Previous studies show that the electrical performance of the HEMT devices is affected very little when the maximum distribution bombarded ions are located deeper than a thin 2DEG layer [28]. Micro-Raman measurements were performed using a Horiba Vlabir with a 532 nm ULF (ultra-low frequency) equipped with a 2048×512 pixels back-illuminated liquid nitrogen-cooled InGaAs array detector. For higher spectral resolution, an 1800 G mm^{-1} grating is used along with a $100\times$, $NA = 0.9$ microscope to focus the laser excitation on the sample and collect the Raman scattered light, resulting in a laser spot size of $\approx 1.0 \mu\text{m}$. Electron transparent specimens were prepared with a Ga^+ focused ion beam (FIB), varying the ion beam current from 21 nA to 72 pA to minimize final FIB damage. TEM and EDX experiments were performed in a 300 kV Tecnai G2 F30 S-TWIN with scanning transmission electron microscopy high-angle annular dark field resolution of 0.17 nm.

3. Results and discussion

The forward saturation current (I_{DS}) starts decreasing from 0.001 dpa during both ON and OFF mode but drastically drops by two orders of magnitude at ON mode, and devices completely lose the forward characteristics at OFF mode after 0.1 dpa as shown in figures 2(a) and (b). The I_{DS} dropped from 328 mA mm^{-1} – 266 mA mm^{-1} , or roughly 19%, when

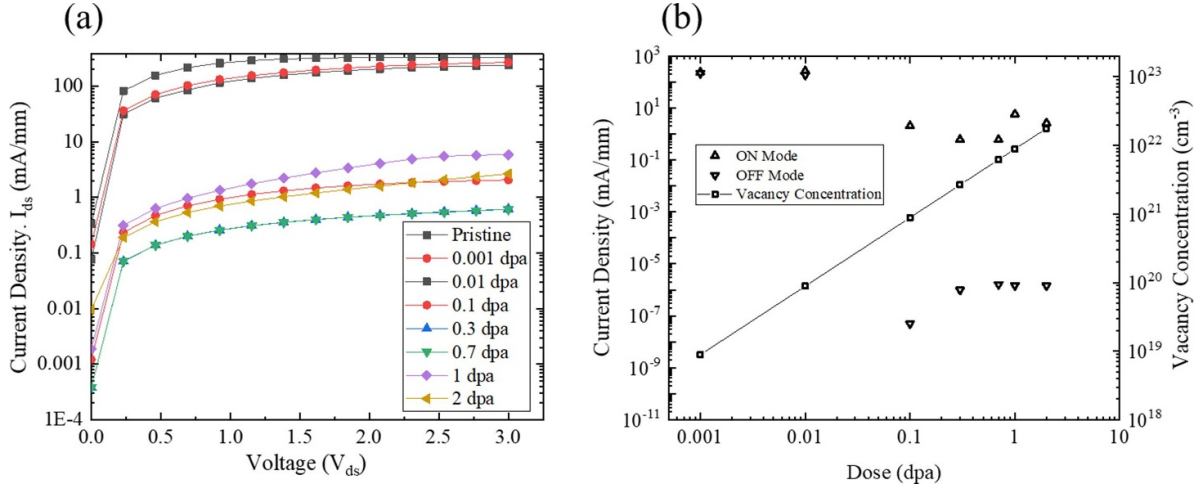


Figure 2. (a) *In situ* I - V characteristics of GaN HEMT at $V_{GS} = 0$ V for ON mode device as a function of dpa. (b) Comparison of saturation current density between ON and OFF mode device operation as a function of dpa.

$V_{GS} = 0$ V and $V_{DS} = 3$ V. Additionally, at low drain voltage, the initial slope of the current curve likewise decreases. When the channel electric field is lower than the critical electric field in AlGaIn/GaN HEMT devices, the current at point x in the 2DEG channel is defined as

$$\frac{I}{w} = qn_s(x)\mu E(x)$$

where q , $n_s(x)$, w , μ , and $E(x)$ denote the mobility, gate's width, the concentration of 2DEG, electron charge, and intensity of the electric field, respectively. Therefore, the declines in initial output curve slope and saturation current reflect a drop in 2DEG density and mobility [29]. The final current density does not scale exactly with the dpa, due to variations in defect recombination rate. The SRIM calculation shows that from the onset of 0.1 dpa (fluence 1.72×10^{12} ions cm^{-2}), saturation current decreases significantly because of the increased inelastic interaction with the lattice resulting from the heavy ion strike, which generates a higher amount of intrinsic lattice defects per ion. The drop in current is a clear sign that there are traps present at the surface and interface of the AlGaIn and GaN layers and displacement damage in the vicinity of the active device region. The generated vacancy concentration is 8.85×10^{20} vacancies cm^{-3} per unit depth according to SRIM simulation (figure 1(b)), and they can function as electron traps and cause the carrier density in 2DEG to decrease. Moreover, heavy atoms like gold can function as impurities and create deep traps if the final position happens to be in the active part of the device. From figure 2(b), we notice that there is a slight recovery of saturation current after 0.7 dpa and 0.1 dpa for ON and OFF mode, respectively. This similar behavior has been observed before with ^{60}Co irradiation in OFF mode [30]. This has been attributed to the fact that the entrapment dynamics of charges generated by irradiation eventually attain equilibrium and compete with the recombination of charge pairs, causing the system to return to its initial state. The current density in the ON-mode device degrades two orders of magnitude after 0.1 dpa whereas the OFF-mode device completely loses its

functionality. It suggests that ON mode operation is more tolerant to irradiation effects than OFF mode, probably due to a more extended annealing period by self-heating during the ON state, providing a way of self-recovery during irradiation [20]. Furthermore, the application of both drain and gate voltage during irradiation can lead to a modification in the behavior of trapped charges due to the presence of horizontal and vertical electric fields. This phenomenon can enhance the robustness of ON mode devices compared to OFF mode devices [22]. The moving electron during ON state can interact with the incoming ion differently than OFF state which can shift the gold ions peak damage depth away from the AlGaIn/GaN layer, leading to an improvement in the radiation hardness of the material.

The ON mode device loses the gate control over forward current after 0.1 dpa, which means negative gate voltage (-3.2 V) can no longer turn off the channel of this GaN HEMT device. The forward resistance of Schottky contact increased by two orders of magnitude after a 2 dpa damage level, as illustrated in figure 3(a). This phenomenon and the complete dysfunctionality of the OFF-state device can be attributed to the sudden increase of leakage current after 0.1 dpa (figure 3(b)). To extract change in Schottky barrier height (SBH) and ideality factor, the thermionic emission model is used for forward current density, which is given by,

$$J = J_s \exp\left(\frac{qV}{nkT} - 1\right) = A^{**}T^2 \exp\left(-\frac{q\phi_{bn}}{kT}\right) \exp\left(\frac{qV}{nkT} - 1\right)$$

where J_s is saturation current density, J is current density, A^{**} is Richardson constant for the metal/semiconductor interface ($26.4 \text{ A cm}^{-2}\text{K}^{-2}$ [31]) and ϕ_{bn} is SBH. Taking log on both sides should produce a line plot for thermionic emission, which can be used to extract the barrier height, ideality factor, and saturation current density. The y-intercept of the $\ln J$ - V curve gives the value of the saturation current density, J_s from which ϕ_{bn} is calculated ($\phi_{bn} = \frac{kT}{q} \ln\left(\frac{A^{**}T^2}{J_s}\right)$) and the ideality factor, n , can be extracted from the slope using the equation

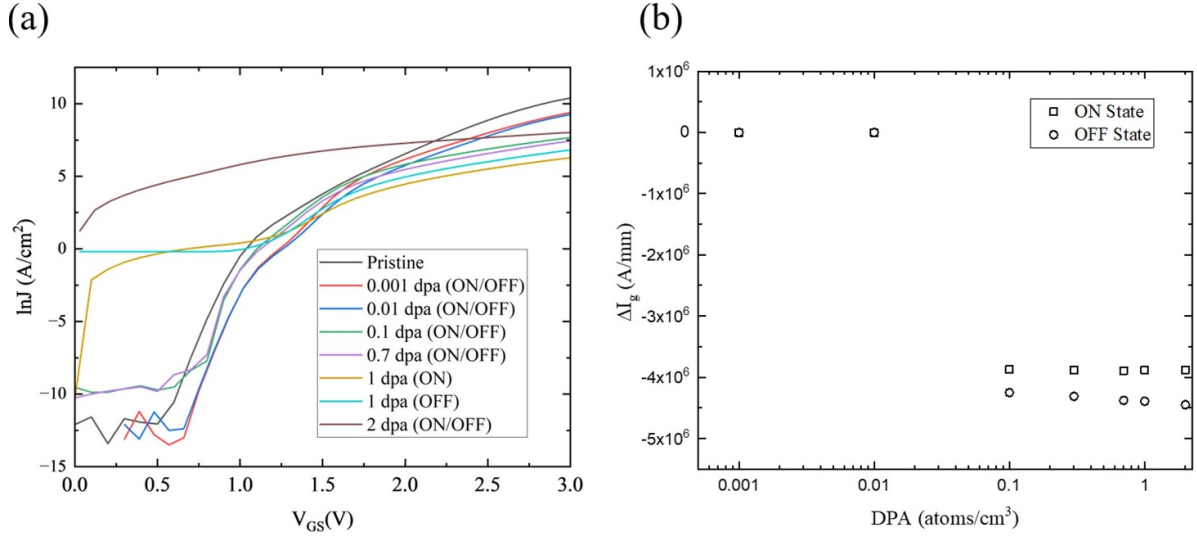


Figure 3. (a) Degradation of Schottky gate forward voltage as a function of operation mode and damage level. (b) Relative increase (compared to pristine condition) of leakage current at ON and OFF mode as a function of damage levels.

$n = \frac{q}{kT} \left(\frac{dV}{d \ln J} \right)$. The extracted values are tabulated below in table 1.

The forward current keeps decreasing with higher fluences as shown in figure 3(a). Initial steady value in the SBH and subsequent decrease after 0.7 dpa is observed from the forward I - V curve. The ON and OFF mode devices show similar n and ϕ_{bn} values except for 1 dpa. The heavy gold ion irradiation introduces interface states at the metal/semiconductor interface, influencing the SBH. A reduction in the height of the barrier suggests an alteration in the electrical characteristics of the interface. These changes may include chemical intermixing that can shift the Fermi energy level pinning for the Schottky contact [32]. The large ideality factor and change SBH indicate various non-idealities, including impurities from gold irradiation at the interface, radiation-induced trap-assisted tunneling current in addition to a thermionic current which eventually leads towards an inhomogeneous metal-semiconductor interface [33]. Gate leakage current exhibited the most significant increase, rising by around six orders of magnitude after 0.1 dpa. Such increase usually occurs for swift heavy ions, which leave latent tracks that act as a leakage path [34]. These results indicate that the Schottky contact has significantly degraded after the ion irradiation. Due to the interfacial trap states and strain-induced defects, such as dislocations and cracks from significant lattice mismatches, the gate reverse leakage current still represents a substantial threat to the stability of GaN-HEMTs, even in pristine conditions [35, 36]. Without causing any radiation damage, the ON-state of a device with a high gate voltage can also contribute to leakage current. By hopping conduction from trap to trap induced by irradiation, tunneling electrons from the gate can produce a leakage current from the gate to the drain. Alternatively, the electrons can travel through the AlGaN layer to the conducting channel or gather on the surface near the gate [37]. The trap-assisted tunneling effects will be enhanced by the nonionizing energy loss (NIEL) of heavy ion-induced defects in the

AlGaN layer that has trapped positive charges and radiation-induced electron traps. They serve as trap-assisted tunneling centers, which eventually cause the gate leakage current to grow. As shown in figure 4(a), the HEMT's transfer properties were assessed with $V_{DS} = 2$ V both before and after being exposed to gold ions. The peak position of the transconductance curve shifts after irradiation, which implies threshold voltage shift has occurred. The deterioration of the transfer characteristics and the positive shift of the threshold voltage address the lowering of the 2DEG density and mobility caused by gold ion radiation-induced defects such as Ga vacancies or N interstitials [38, 39]. At the lowest fluence (0.001 dpa), we observe V_{th} shift from -2.8 V to -2.68 V and 40.14% decrease in transconductance (g_m). After 0.01 dpa, V_{th} shifted further positive to -2.6 V, but transconductance increased by 17% compared to 0.001 dpa. The increase in the transconductance can be attributed to the irradiation-induced strain relaxation AlGaN/GaN HEMTs, which occur at lower fluence [6, 28, 40]. During ion irradiation, both donor and acceptor trap creation had been reported [24, 28, 41]. The increase in acceptor-like trap density is responsible for the positive V_{th} shift at low gold ion fluence. Both ON and OFF mode operations show similar degradation at low fluences, and after 0.01 dpa, gate control over the channel is completely lost, hence no V_{th} or g_m is available.

The typical Raman scattering spectra of the pristine and gold ion-irradiated samples that are collected at room temperature are shown in figure 4(b). No significant distinction has been observed in the Raman spectra between devices operating in ON and OFF modes. In the experiment, the E_2 (High) and A_1 (LO) modes for GaN were observed using the $z(-, -)z$ back scattering geometry. Comparing the irradiation sample to the pristine samples, the peak intensities were lesser for the irradiated samples. The frequency of E_2 (High) phonon mode did not change after irradiation; however, there is a slight shift in the frequency position towards the lower

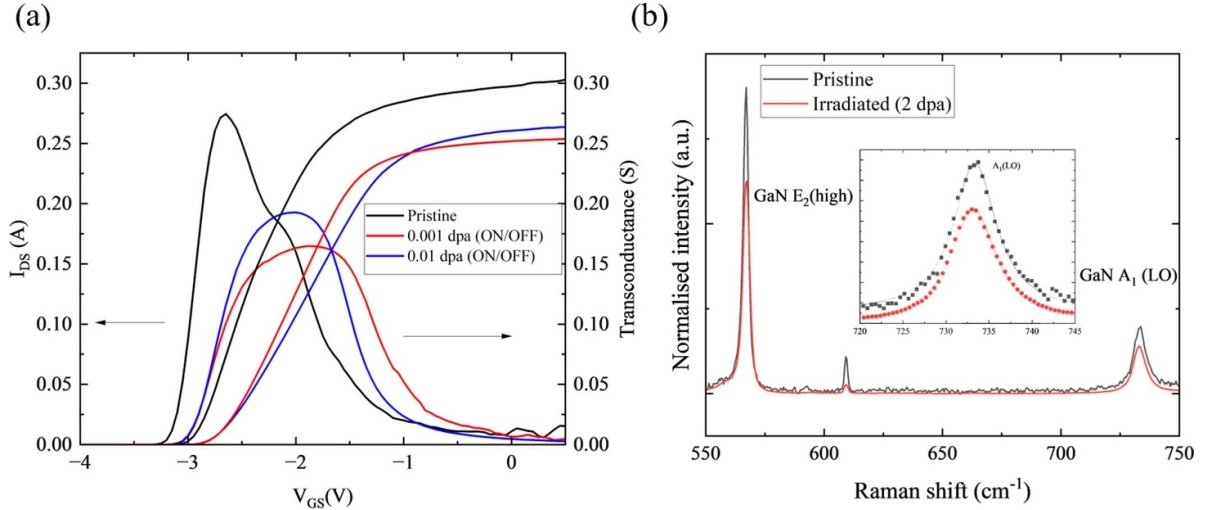


Figure 4. (a) Transfer characteristics and transconductance and (b) Raman spectra of the pristine and 2 dpa irradiated samples (ON/OFF).

Table 1. Ideality factor and SBH as function of dpa of Ni/Au Schottky contact in AlGaIn/GaN HEMT. Gate area is $1.2 \text{ mm} \times 0.25 \text{ }\mu\text{m}$.

	Pristine	0.001 dpa	0.01 dpa	0.1 dpa	0.7 dpa	1 dpa	2 dpa	
	ON/OFF	ON/OFF	ON/OFF	ON/OFF	ON/OFF	ON	OFF	ON/OFF
Ideality factor	1.44	1.37	1.44	1.24	1.34	6.34	5.44	12.24
Barrier height (eV)	1.15	1.18	1.15	1.21	1.16	0.45	0.58	0.45

wavenumber (from 733.38 cm^{-1} to 733.02 cm^{-1}) and a slight increase (from 6.11 cm^{-1} to 6.6 cm^{-1}) in the full width at half maximum (FWHM) of irradiated samples in reference to the pristine sample for $A_1(\text{LO})$ modes. The $A_1(\text{LO})$ peak is fitted with Lorentzian fit assuming negligible spectrometer-induced broadening. It can be assumed that 2.8 MeV Au^{4+} irradiation has caused a strain relaxation in the heterostructure based on the slight shift of the Raman phonon mode to a lower wavenumber [42]. The broadening of FWHM of $A_1(\text{LO})$ suggests a decrease in phonon lifetime according to energy-time uncertainty principle. The phonon lifetimes are primarily regulated by two mechanisms, namely the anharmonic interactions among phonons resulting in the decay of a phonon into other phonons and the scattering of phonons at impurity or defect centers. As the experiment is done at room temperature, phonon-phonon interaction will have less effect on phonon lifetime. Defects created by gold irradiation can function as scattering centers for phonons, which disrupts their propagation and causes them to decay more quickly.

To obtain further physical evidence of GaN HEMT device degradation, we performed high-resolution transmission electron microscopy (HRTEM) analysis close to the interface of AlGaIn/GaN in both ON and OFF mode devices. SRIM measurements indicate that the range of a 2.8 MeV gold ion in bulk GaN HEMT is only $0.62 \text{ }\mu\text{m}$, which does not entirely penetrate the device structure. All gold ions remain in the GaN layer to function as trap states. The energetic gold ions displace Al, Ga, and N atoms, and the recoil energy of the displaced atoms translates to a certain knock-on distance. This suggests that

an inherent intermixing is expected at the 2DEG layer. SRIM simulation also shows that the Al, Ga, and N profile in the AlGaIn barrier layer is broadened by almost 20 nm , and this broadening is expected to contribute to the irradiated HEMT's interfacial roughening which also leads to electrical property degradation [43]. This radiation-induced atomic intermixing is demonstrated in figures 5(a) and (b) by comparing HRTEM images of pristine and OFF mode ion irradiated samples, respectively. The AlGaIn/GaN interface is abrupt in pristine condition, as seen in figure 5(a), which is a requirement for HEMT to maintain a piezoelectric field at the interface. Without the piezoelectric effect, the HEMT is depleted near the interfaces, preventing it from attaining high electron mobility and sheet carrier density [44]. After 2 dpa irradiation damage, both ON and OFF mode devices show less abrupt AlGaIn/GaN interfaces due to interfacial roughening and intermixing, as shown in figure 5(b). This atomic disorder in the crystalline interface also associates point defects which can scatter carriers or act like acceptors (such as Al vacancies) in the 2DEG layer and degrade electrical performance [32]. This similar kind of interface roughening is also observed in proton irradiation with energy close to 2 MeV [45]. They found substantially less broadening of the Al peak because proton ions cannot create large, kinematically favored cascades like gold ions. Geometrical phase analysis offers mapping of strain at nanoscale precision from HRTEM images of pristine and irradiated samples. This method highlights the extent of radiation damage in atoms that are slightly away from equilibrium compared to the regular lattice in the AlGaIn or GaN layers. We

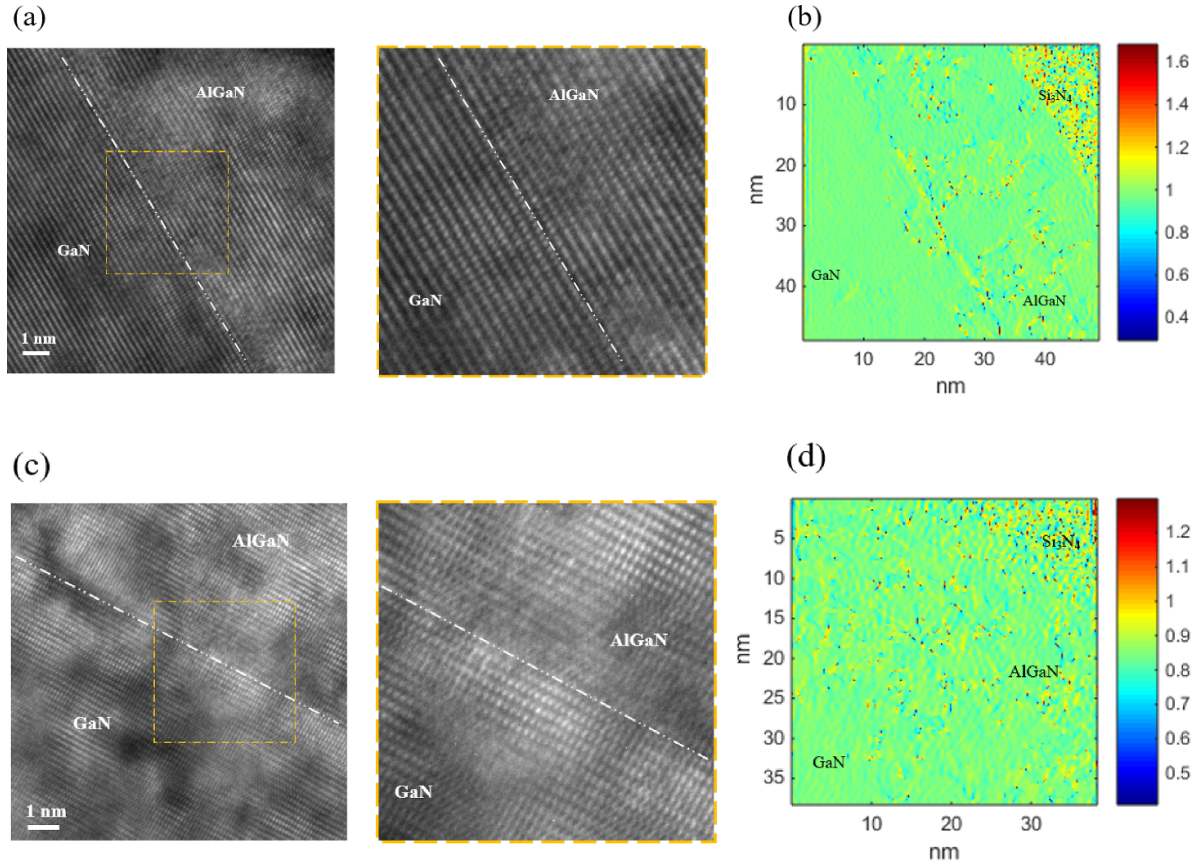


Figure 5. High-resolution STEM image of the GaN/AlGaIn interface of pristine (a) and ion irradiated (c) of 3.745×10^{13} ions cm^{-2} (2 dpa OFF mode). The interface is less abrupt after irradiation. (b) and (d) are the GPA analysis of GaN HEMT's HRTEM of pristine and ion irradiated with Si_3N_4 /AlGaIn/GaN interfaces. The scale bar represents strain value in percent (the value range of the scale bar is different for each image).

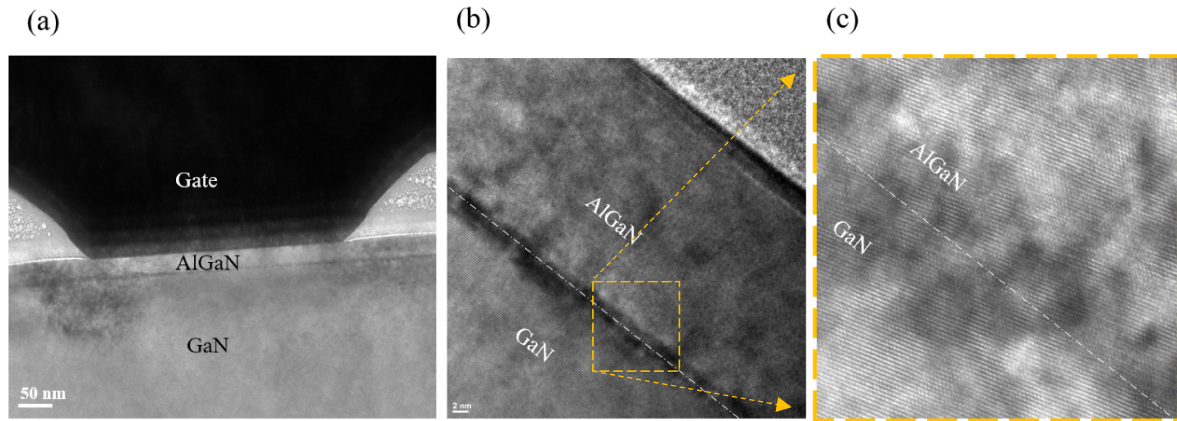


Figure 6. ON mode GaN HEMT (a) cross-sectional TEM image near gate terminal (b) and (c) show the interface region where irradiation-induced defects are primarily formed.

find atomic defects in both pristine and irradiated interfaces. However, the AlGaIn-GaN interface experiences strain relaxation and higher defect concentration after irradiation. Defects propagated into the GaN layer after irradiation as displacement damage occurs primarily at the end of the 2.8 MeV Au^{4+} range in the device. The ON mode device shows further degradation

(figure 6(a)) near the gate edge, where the highest electric field is generated when the gate voltage is applied. This implies that the highly stressed region is more vulnerable to incoming radiation [6]. The degradation observed in figures 6(b) and (c) for the interface in the ON-mode device is also similar to that observed in the OFF-mode device.

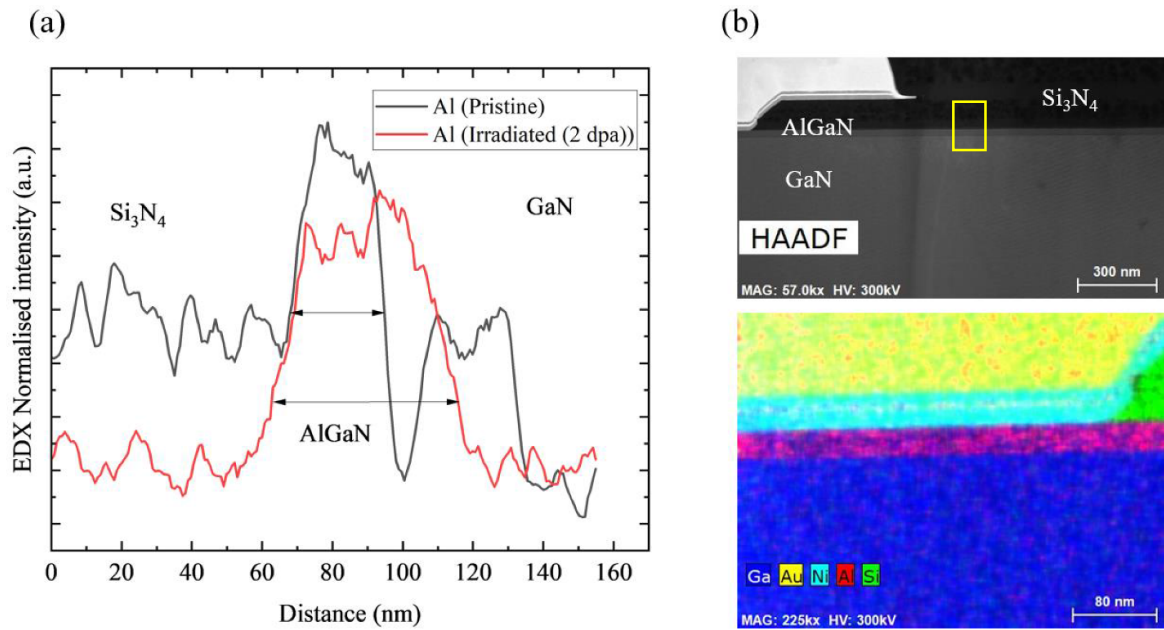


Figure 7. (a) EDS box scan through a cross-section of the HEMT before and after the highest dose of Au^{4+} radiation in this study. (b) HAADF image of the GaN/AlGaIn interface after the highest fluence of Au^{4+} radiation. The yellow box is where the box scan is performed to get the Al profile. The bottom shows an overlay EDX image near the interface.

We see from figure 1(b) that electronic stopping powers (ionizing energy loss) are much larger than the nuclear-stopping power (non-ionizing energy loss) of 2.8 MeV gold ions in the GaN HEMT structure. Therefore, electronic energy loss processes have minimal impact on the formation of defects in GaN during gold ion bombardment. Most defects were generated by the NIEL events which are recorded as vacancies, interstitials, and multiple defect complexes. As those defects build up, they start to move or diffuse. They can be transported ballistically by more incoming ion bombardment or move by diffusion mechanisms and eventually find each other, forming clusters. The vacancy production is proportional to irradiation fluence (figure 2(b)), and Ga vacancies are produced in maximum number in GaN HEMT devices after 2.8 MeV Au^{4+} irradiation according to the SRIM simulations. The findings of SRIM only consider the creation of defects, not the immediate relaxation or long-term evolution. Because of very high formation energy, many defect structures produced by irradiation are unstable [46]. GaN HEMT exhibits a powerful dynamic annealing effect, suggesting that most defects may be eliminated or recombined with vacant sites. One MD simulation findings show 96% of defects recombine with vacancies after 30 MeV fluorine ion irradiation [47]. Hence, it is difficult to find significant signs of defects in HRTEM analysis.

Energy dispersive x-ray (EDX) box scan (figure 7(b)) perpendicular to the AlGaIn/GaN interface further reveals radiation-induced atomic intermixing/disorder. As illustrated in figure 7(a), we found the Al profile broadening (~ 20 nm) into the GaN layer after irradiation. Al broadening is expected to be accompanied by a broadening of the Ga and N. The broadening of Ga and N cannot be resolved because the

AlGaIn layer is next to a GaN layer. Still, it is anticipated that this broadening will also contribute to the interfacial roughening and deterioration of the electrical characteristics of the irradiated HEMT [43]. As a result of the gold ion impact, atoms in the device that experience strong recoil energies will be knocked off the original lattice site causing a chain reaction of more collisions and hence, more atomic intermixing. Kinchin–Pease formula-based model (SRIM) also predicted elemental broadening in the AlGaIn layer and N atom from Si_3N_4 into the AlGaIn layer. Both occurrences have the potential to drastically change the properties of AlGaIn, resulting in a decrease in transport properties.

Due to inadequate knowledge of the process of defect nucleation and propagation because of applied and inherent stress in the devices, long-term device reliability for post-irradiated electronics remains a challenge. The wide variety of applications for GaN HEMTs may be ensured by a more thorough investigation opening the door to understanding the damage physics under radiation and various localized stressors including operating conditions (ON, semi-ON, pinched off), temperature and electrically pre-stressed conditions. This study investigated these effects on GaN HEMTs with field plates that mitigate highly localized electric fields. We believe that the fundamental understanding could still be extrapolated to the devices without field plates. Our hypothesis is that the absence of field plates will induce more sensitivity to radiation damage. This is because high electrical field over time nucleates atomic scale structural defects. These defects function as ‘pre-existing conditions’ upon incoming radiation. Since the local lattice is already distorted, it is easier for the energetic particles to inflict more damage.

4. Conclusion

In conclusion, 2.8 MeV Au⁴⁺ radiation damage in AlGaIn/GaN HEMTs has been systematically investigated as a function of radiation dose or dpa and two operating conditions: ON and OFF. When irradiated up to a fluence of 1.72×10^{11} ions cm⁻² (0.01 dpa), gate control over the channel is retained; however, decreases in saturation drain current, maximum transconductance, a shift in threshold voltage, and an increased leakage current are observed in both ON and OFF modes. These are contributed to the decline of carrier density or mobility, displacement damage close to the active device region, and an increase in acceptor-like trap density. The devices degraded severely from 1.72×10^{12} ions cm⁻² fluence with high gate leakage, increased forward current resistance, and lost Schottky behavior of the gate contact. Atomic disorder in AlGaIn/GaN interface and higher defects in the GaN layer associated with strain relaxation have been attributed to the failure of these devices. ON devices show higher radiation tolerance than OFF modes due to a more extended annealing period by self-heating, providing a way of self-recovery during irradiation. Micro-Raman confirmed reduced crystal quality and strain modification after irradiation. HRTEM and EDX are used to analyze the sample's interfacial roughening caused by displacement damage after the highest irradiation fluence for the experiment.

Data availability statement

The data cannot be made publicly available upon publication because they are not available in a format that is sufficiently accessible or reusable by other researchers. The data that support the findings of this study are available upon reasonable request from the authors.

Acknowledgments

This work was funded by the Defense Threat Reduction Agency (DTRA) as part of the Interaction of Ionizing Radiation with Matter University Research Alliance (IIRM-URA) under contract number HDTRA1-20-2-0002. Aman Haque also acknowledges support from the US National Science Foundation (ECCS # 2015795). The content of the information does not necessarily reflect the position or the policy of the federal government, and no official endorsement should be inferred. The work at UF was also supported by NSF DMR 1856662. This work was performed, in part, at the Center for Integrated Nanotechnologies, an Office of Science User Facility operated for the U.S. Department of Energy (DOE) Office of Science. Sandia National Laboratories is a multi-mission laboratory managed and operated by National Technology & Engineering Solutions of Sandia, LLC, a wholly owned subsidiary of Honeywell International, Inc., for the U.S. DOE's National Nuclear Security Administration under contract DE-NA-0003525. The views expressed in the article do not necessarily represent the views of the U.S. DOE or the United States Government.

ORCID iDs

C Thomas Harris  <https://orcid.org/0000-0003-4946-7181>
 Aman Haque  <https://orcid.org/0000-0001-6535-5484>
 Stephen J Pearton  <https://orcid.org/0000-0001-6498-1256>

References

- [1] Fleetwood D M, Zhang E X, Schrimpf R D and Pantelides S T 2022 Radiation effects in AlGaIn/GaN HEMTs *IEEE Trans. Nucl. Sci.* **69** 1105–19
- [2] Pearton S et al 2021 Radiation damage in wide and ultra-wide bandgap semiconductors *ECS J. Solid State Sci. Technol.* **10** 055008
- [3] Ionascut-Nedelcescu A, Carlone C, Houdayer A, Von Bardeleben H, Cantin J-L and Raymond S 2002 Radiation hardness of gallium nitride *IEEE Trans. Nucl. Sci.* **49** 2733–8
- [4] Nordlund K, Ghaly M, Averback R, Caturla M, de La Rubia T D and Tarus J 1998 Defect production in collision cascades in elemental semiconductors and FCC metals *Phys. Rev. B* **57** 7556
- [5] Del Alamo J A and Joh J 2009 GaN HEMT reliability *Microelectron. Reliab.* **49** 1200–6
- [6] Rasel M A J, Stepanoff S P, Wetherington M, Haque A, Wolfe D E, Ren F and Pearton S 2022 Thermo-mechanical aspects of gamma irradiation effects on GaN HEMTs *Appl. Phys. Lett.* **120** 124101
- [7] Pearton S, Hwang Y-S and Ren F 2015 Radiation effects in GaN-based high electron mobility transistors *JOM* **67** 1601–11
- [8] Bazzoli S, Girard S, Ferlet-Cavrois V, Baggio J, Paillet P and Duhamel O 2007 SEE sensitivity of a COTS GaN transistor and silicon MOSFETs 2007 9th European Conf. on Radiation and Its Effects on Components and Systems (IEEE) pp 1–5
- [9] Kuboyama S, Maru A, Shindou H, Ikeda N, Hirao T, Abe H and Tamura T 2011 Single-event damages caused by heavy ions observed in AlGaIn/GaN HEMTs *IEEE Trans. Nucl. Sci.* **58** 2734–8
- [10] Rostewitz M, Hirche K, Lätti J and Jutzi E 2013 Single event effect analysis on DC and RF operated AlGaIn/GaN HEMTs *IEEE Trans. Nucl. Sci.* **60** 2525–9
- [11] Lei Z, Guo H X, Tang M H, Zeng C, Zhang Z G, Chen H, En Y F, Huang Y, Chen Y Q and Peng C 2018 Degradation mechanisms of AlGaIn/GaN HEMTs under 800 MeV bi ions irradiation *Microelectron. Reliab.* **80** 312–6
- [12] Islam Z, Paoletta A L, Monterrosa A M, Schuler J D, Rupert T J, Hattar K, Glavin N and Haque A 2019 Heavy ion irradiation effects on GaN/AlGaIn high electron mobility transistor failure at off-state *Microelectron. Reliab.* **102** 113493
- [13] Liu L et al 2013 Dependence on proton energy of degradation of AlGaIn/GaN high electron mobility transistors *J. Vac. Sci. Technol. B* **31** 022201
- [14] Polyakov A Y, Pearton S, Frenzer P, Ren F, Liu L and Kim J 2013 Radiation effects in GaN materials and devices *J. Mater. Chem.* **1** 877–87
- [15] Hu X, Choi B K, Barnaby H J, Fleetwood D M, Schrimpf R D, Lee S, Shojah-Ardalan S, Wilkins R, Mishra U K and Dettmer R W 2004 The energy dependence of proton-induced degradation in AlGaIn/GaN high electron mobility transistors *IEEE Trans. Nucl. Sci.* **51** 293–7
- [16] Sequeira M C et al 2021 Unravelling the secrets of the resistance of GaN to strongly ionising radiation *Commun. Phys.* **4** 1–8

- [17] Cai S *et al* 2000 Annealing behavior of a proton irradiated Al/sub x/Ga/sub 1-x/N/GaN high electron mobility transistor grown by MBE *IEEE Trans. Electron Devices* **47** 304–7
- [18] Hu X *et al* 2003 Proton-irradiation effects on AlGaN/AlN/GaN high electron mobility transistors *IEEE Trans. Nucl. Sci.* **50** 1791–6
- [19] Lei Z, Guo H, Tang M, Peng C, Zhang Z, Huang Y and En Y 2018 Mechanism of high-fluence proton induced electrical degradation in AlGaN/GaN high-electron-mobility transistors *Jpn. J. Appl. Phys.* **57** 074101
- [20] Rasel M A J, Stepanoff S, Haque A, Wolfe D E, Ren F and Pearton S J 2022 Gamma radiation on gallium nitride high electron mobility transistors at ON, OFF, and prestressed conditions *J. Vac. Sci. Technol. B* **40** 063204
- [21] Chen R, Liang Y, Han J, Lu Q, Chen Q, Wang Z, Wang H, Wang X and Yuan R 2022 Research on the synergistic effect of total ionization and displacement dose in GaN HEMT using neutron and gamma-ray irradiation *Nanomaterials* **12** 2126
- [22] Bôas A C V, de Melo M A A, Santos R B B, Giacomini R, Medina N H, Seixas L E, Finco S, Palomo F R, Romero-Maestre A and Guazzelli M A 2021 Ionizing radiation hardness tests of GaN HEMTs for harsh environments *Microelectron. Reliab.* **116** 114000
- [23] Martínez P J, Maset E, Martín-Holgado P, Morilla Y, Gilabert D and Sanchis-Kilders E 2019 Impact of gamma radiation on dynamic RDSON characteristics in AlGaIn/GaN power HEMTs *Materials* **12** 2760
- [24] Jiang R *et al* 2016 Worst-case bias for proton and 10-keV x-ray irradiation of AlGaIn/GaN HEMTs *IEEE Trans. Nucl. Sci.* **64** 218–25
- [25] Pengelly R S, Wood S M, Milligan J W, Sheppard S T and Pribble W L 2012 A review of GaN on SiC high electron-mobility power transistors and MMICs *IEEE Trans. Microw. Theory Tech.* **60** 1764–83
- [26] Hattar K M, Bufford D C, Marshall M T, Doyle B L and Buller D L 2014 *Development of a Concurrent In situ Ion Irradiation TEM* (Albuquerque, NM: Sandia National Lab. (SNL-NM))
- [27] Ziegler J F, Ziegler M D and Biersack J P 2010 SRIM—the stopping and range of ions in matter (2010) *Nucl. Instrum. Methods Phys. Res. B* **268** 1818–23
- [28] Khanal M P *et al* 2018 Impact of 100 keV proton irradiation on electronic and optical properties of AlGaIn/GaN high electron mobility transistors (HEMTs) *J. Appl. Phys.* **124** 215702
- [29] Turuvekere S, Karumuri N, Rahman A A, Bhattacharya A, DasGupta A and DasGupta N 2013 Gate leakage mechanisms in AlGaIn/GaN and AlInN/GaN HEMTs: comparison and modeling *IEEE Trans. Electron Devices* **60** 3157–65
- [30] Bôas A C V *et al* 2021 Reliability analysis of gamma-and x-ray TID effects, on a commercial AlGaIn/GaN based FET *J. Integr. Circuits Syst.* **16** 1–7
- [31] Schmitz A, Ping A, Khan M A, Chen Q, Yang J and Adesida I 1996 Schottky barrier properties of various metals on n-type GaN *Semicond. Sci. Technol.* **11** 1464
- [32] White B, Bataiev M, Goss S H, Hu X, Karmarkar A, Fleetwood D M, Schrimpf R D, Schaff W J and Brillson L J 2003 Electrical, spectral, and chemical properties of 1.8 MeV proton irradiated AlGaIn/GaN HEMT structures as a function of proton fluence *IEEE Trans. Nucl. Sci.* **50** 1934–41
- [33] Werner J H and Güttler H H 1991 Barrier inhomogeneities at Schottky contacts *J. Appl. Phys.* **69** 1522–33
- [34] Lei Z-F, Guo H-X, Zeng C, Chen H, Wang Y-S and Zhang Z-G 2015 Influence of heavy ion irradiation on DC and gate-lag performance of AlGaIn/GaN HEMTs *Chin. Phys. B* **24** 056103
- [35] Mimouni A, Fernández T, Rodríguez-Tellez J, Tazón A, Baudrand H and Boussuis M 2012 Gate leakage current in GaN HEMT's: a degradation modeling approach *Electr. Electron. Eng.* **2** 397–402
- [36] Besendörfer S, Meissner E, Medjdoub F, Derluyn J, Friedrich J and Erlbacher T 2020 The impact of dislocations on AlGaIn/GaN Schottky diodes and on gate failure of high electron mobility transistors *Sci. Rep.* **10** 1–12
- [37] Trew R, Liu Y, Kuang W and Bilbro G 2006 The physics of reliability for high voltage AlGaIn/GaN HFET's 2006 *IEEE Compound Semiconductor Integrated Circuit Symp.* (IEEE) pp 103–6
- [38] Liu L, Hwang Y-H, Xi Y, Ren F, Craciun V, Pearton S J, Yang G, Kim H-Y and Kim J 2014 Study on the effects of proton irradiation on the dc characteristics of AlGaIn/GaN high electron mobility transistors with source field plate *J. Vac. Sci. Technol. B* **32** 022202
- [39] Pearton S, Ren F, Patrick E, Law M and Polyakov A Y 2015 Ionizing radiation damage effects on GaN devices *ECS J. Solid State Sci. Technol.* **5** Q35
- [40] Lee J *et al* 2017 Low dose 60Co gamma-irradiation effects on electronic carrier transport and DC characteristics of AlGaIn/GaN high-electron-mobility transistors *Radiat. Eff. Defects Solids* **172** 250–6
- [41] Kim D-S, Lee J-H, Kim J-G, Yoon Y J, Lee J S and Lee J-H 2020 Anomalous DC characteristics of AlGaIn/GaN HEMTs depending on proton irradiation energies *ECS J. Solid State Sci. Technol.* **9** 065005
- [42] Kurakin A, Vitusevich S A, Danylyuk S V, Hardtdegen H, Klein N, Bougrioua Z, Danilchenko B A, Konakova R V and Belyaev A E 2008 Mechanism of mobility increase of the two-dimensional electron gas in AlGaIn/GaN heterostructures under small dose gamma irradiation *J. Appl. Phys.* **103** 083707
- [43] Patrick E E, Choudhury M, Ren F, Pearton S J and Law M E 2015 Simulation of radiation effects in AlGaIn/GaN HEMTs *ECS J. Solid State Sci. Technol.* **4** Q21
- [44] Zhang Y and Singh J 1999 Charge control and mobility studies for an AlGaIn/GaN high electron mobility transistor *J. Appl. Phys.* **85** 587–94
- [45] Greenlee J D, Specht P, Anderson T J, Koehler A D, Weaver B D, Luysberg M, Dubon O D, Kub F J, Weatherford T R and Hobart K D 2015 Degradation mechanisms of 2 MeV proton irradiated AlGaIn/GaN HEMTs *Appl. Surf. Sci.* **107** 083504
- [46] Limpijumngong S and Van de Walle C G 2004 Diffusivity of native defects in GaN *Phys. Rev. B* **69** 035207
- [47] Wan P *et al* 2022 The study of displacement damage in AlGaIn/GaN high electron mobility transistors based on experiment and simulation method *IEEE Trans. Nucl. Sci.* **69** 1120–6